

Nonisothermal crystallization kinetics of novel biodegradable poly(butylene succinate-*co*-2-methyl-1,3-propylene succinate)s

Jin-Shan Lu · Ming Chen · Shih-Fu Lu · Chi-He Chen

Received: 15 October 2010 / Accepted: 21 December 2010 / Published online: 8 January 2011
© Springer Science+Business Media B.V. 2011

Abstract Two novel poly(butylene succinate-*co*-2-methyl-1,3-propylene succinate)s, PBMPsu 95/5 and PBMPsu 90/10, were characterized as having 6.5 and 10.8 mol% 2-methyl-1,3-propylene succinate (MS) units, respectively, by ¹H NMR. A differential scanning calorimeter (DSC) and a polarized light microscope (PLM) employed to investigate the nonisothermal crystallization of these copolyesters and poly(butylene succinate) (PBSu). Morphology and the isothermal growth rates of spherulites under PLM experiments at three cooling rates of 1, 2.5 and 5 °C/min were monitored and obtained by curve-fitting. These continuous rate data were analyzed with the Lauritzen-Hoffman equation. A transition of regime II→III was found at 96.2, 83.5, and 77.9 °C for PBSu, PBMPsu 95/05, and PBMPsu 90/10, respectively. DSC exothermic curves at five cooling rates of 1, 2.5, 5, 10 and 20 °C/min show that almost all of the nonisothermal crystallization occurred in regime III. DSC data were analyzed using modified Avrami, Ozawa, Mo, Friedman and Vyazovkin equations. All the results of PLM and DSC measurements reveal that incorporation of minor MS units into PBSu markedly inhibits the crystallization of the resulting polymer.

Keywords Crystallization · Differential scanning calorimetry (DSC) · Morphology · Polyesters

Electronic supplementary material The online version of this article (doi:10.1007/s10965-010-9558-2) contains supplementary material, which is available to authorized users.

J.-S. Lu · M. Chen (✉) · S.-F. Lu · C.-H. Chen
Department of Materials and Optoelectronic Science,
National Sun Yat-Sen University,
Kaohsiung 80424,
Taiwan, Republic of China
e-mail: mingchen@mail.nsysu.edu.tw

Introduction

In recent years, the use in a large amount of the chemosynthetic polymers has caused a global environmental problem because these polymers are difficult to be decomposed. Biodegradable polymers which can be degraded to CH₄, CO₂ and H₂O by enzymes or microorganisms have received much attention as ecological materials [1]. Aliphatic polyesters have been a good choice among many biodegradable polymers. Poly(butylene succinate) (PBSu) which is a chemosynthetic aliphatic polyester has relatively high melting point and comparable mechanical properties with those of widely used polymers such as low-density polyethylene (LDPE) and poly(propylene) [2]. Because it can be processed using conventional equipments, it becomes the hopeful substitute for LDPE.

Fundamentally, the characterization for the enzymatic degradation of polyester films demonstrated that the degree of crystallinity, morphology and crystal structure play an important role in the mechanical properties and biodegradability of polymers [3]. In many literatures, the crystalline structure, crystallization and melting behavior of neat PBSu [4–15] have been investigated extensively. PBSu has a relatively low biodegradation rate because of its high crystallization rate and high crystallinity. To improve the biodegradability of PBSu, physical blending and copolymerization have often been adopted. About copolymers, the degradation rates of PBSu can be increased by incorporating minor amounts of diols or diacids [10, 16, 17] because of the reduced crystallinity.

Poly(propylene succinate) (PPSu) derived from 1,3-propanediol with an odd number of carbon atoms in the backbone has gained increasing attention, because it has a higher biodegradation rate than that with two or four carbon atoms in the diol monomer [18–20]. Poly(butylene succinate-*co*-propylene succinate) (PBPSu) copolymers

have been synthesized and characterized by combining PBSu with a high melting point and PPSu with high biodegradability [21–25]. The crystallization rate of PBPSu decreases as the mol% of propylene succinate unit increases.

In contrast with the high cost and the limited availability of 1,3-propanediol, 2-methyl-1,3-propanediol (MPD) is commercially available in early 1990s. It is well known that the linearity and conformation of polymer backbone have a significant effect on the crystallization behavior of the polymer. Upon introducing the MPD units into the backbone, methyl group on the side chain of a polymer will further retard the crystallization [26–30]. No earlier study of PBSu-based copolymers involving MPD units could be found in the literatures. Furthermore, the crystallization kinetics under nonisothermal conditions has not been studied.

In a previous study [31], PBSu and PBSu-rich copolyesters [poly(butylene succinate-co-2-methyl-1,3-propylene succinate), PBMPSu] with high molecular weight were synthesized via a direct polycondensation reaction in the presence of a highly effective catalyst, titanium tetraisopropoxide. The distribution of 2-methyl-1,3-propylene succinate (MS) unit in these copolymers was characterized to be random from the ^{13}C NMR spectrum. The heating thermograms of quenched specimens and the WAXD patterns of melt-crystallized specimens show that incorporating MS units into PBSu markedly inhibits its crystallization rate.

In this study, the growth rates and the morphology of spherulites were obtained by performing nonisothermal experiments under a polarized light microscope (PLM). Three cooling rates (ϕ) of 1, 2.5 or 5 °C/min were employed. Curve-fitting methods allow the isothermal growth rates of PBSu and PBMPSu spherulites to be determined. Continuous growth rates were analyzed using the Lauritzen–Hoffman (LH) equation [32]. Nonisothermal crystallization of PBSu and its PBMPSu copolymers was also examined using a differential scanning calorimeter (DSC) at five different cooling rates. A time-temperature-transformation (TTT) diagram was superposed on the continuous-cooling-transformation (CCT) curves of PBSu and its copolymers [33]. The crystallization kinetics of the exothermic enthalpy were analyzed and compared using modified Avrami [34–36], Ozawa [37], and Mo [38] models. Finally, the activation energy of crystallization was evaluated using the isoconversional methods of Friedman [39] and Vyazovkin [40, 41]. These results are compared with the results of kinetics studies.

Experimental

Materials and preparation of specimens

PBSu and PBSu-rich copolymers with minor amounts of MS units were synthesized by a two-stage esterification

reaction of succinic acid, 1,4-butanediol (BD) and MPD [31]. The copolyesters used in this study are PBMPSu 95/05 and PBMPSu 90/10 where the numerical values represent the feed ratios of the diols (BD/MPD).

NMR spectra of *d*-chloroform solutions were obtained using tetramethylsilane as the reference standard on a Varian UNITY INOVA-500 NMR at 295.5 K. Figure 1 displays the ^1H NMR spectrum of the PBMPSu 90/10 copolymer and the peak assignments. The two chemical shifts at 4.09–4.15 and 1.68–1.74 ppm are associated with the methylene protons that are α (H_1) and β (H_2) bonded to the ester oxygen in the butylene succinate (BS) units. The chemical shift of the protons of the succinic moiety (H_3) appears at 2.61–2.66 ppm, whereas those of the H_4 , H_5 and H_6 protons derived from the MPD monomer are at $\delta=4.01$ –4.06, 2.12–2.22 and 0.97–1.01 ppm, respectively. A magnified view of the protons is presented in the inset spectra in Fig. 1. H_1 , H_4 and H_5 appear as triplet, doublet and octet, respectively. The compositions of these copolymers were determined from the relative integration areas under the proton peaks of BS and MS units. The mol% ratio of BS/MS in PBMPSu 95/05 was 93.5/6.5. That in PBMPSu 90/10 was characterizing as having 89.2/10.8. The analysis of the ^{13}C NMR spectra of the carbonyl carbon indicates a random distribution of the comonomers in these two copolymers [31].

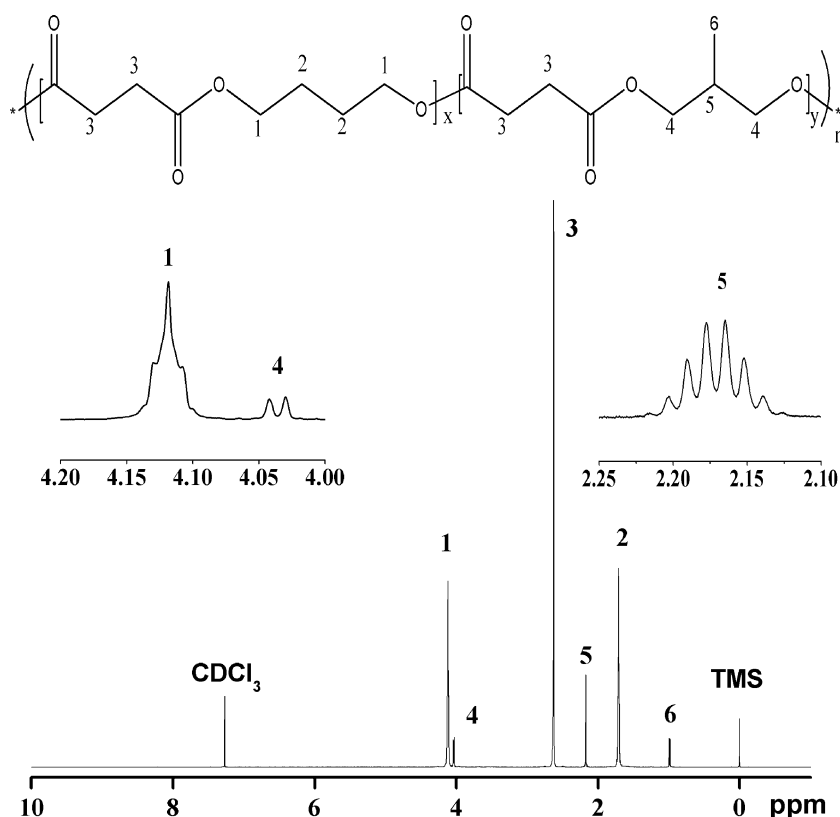
The number average molecular weight of PBSu, PBMPSu 95/05, and PBMPSu 90/10 were 3.0×10^4 , 2.7×10^4 , and 2.4×10^4 g/mol, respectively, relative to poly(methyl methacrylate) which were obtained from gel permeation chromatography at 40 °C using hexafluoroisopropanol as the solvent [31]. Their molecular weight distribution values were 2.5, 2.7 and 2.2. The corresponding values of glass transition temperature (T_g) were -41.1 , -39.9 and -38.3 °C, respectively, and those of melting temperatures (T_m) were 113.1, 107.4 and 102.5 °C, respectively, which were measured at 10 °C/min using a Perkin-Elmer Pyris 1 DSC [31].

Dried polyesters were sandwiched between two polyimide films and two copper plates which were then hot pressed at a preset temperature 20–30 °C above T_m under 2.5 and 5 kg/cm² pressure. Compressed sheets with a thickness of about 0.2 mm were made and then dried *in vacuo* overnight at room temperature before use.

PLM measurements

The spherulites growth rates of polyesters were determined by a Nikon Optiphot-pol polarizing microscope which equipped with a Linkam THMS-600 heating stage and a TMS-91 temperature controller. The video photograph system was adopted with a Sony DXC-755 CCD color video camera, a Pioneer DVR-510H DVD recorder and a

Fig. 1 ^1H NMR spectrum of PBMPsu 90/10 (solvent: *d*-chloroform at 295.5 K) and its peak assignments



Nikon COOLPIX P510 digital camera. Fresh specimen was sandwiched between two microscopic covers and heated at 20 °C/min under nitrogen to 70–80 °C above melting temperature, at which temperature it was maintained for 5 min to melt the crystalline residues. In the nonisothermal experiment, the premolten specimen of PBSu was cooled rapidly from 190 to 89 °C (to 87 °C for PBMPsu 95/05 and 85 °C for PBMPsu 90/10, respectively), held for 4 min for the development of nuclei, heated at 100 °C/min to 99 °C (to 97 °C for PBMPsu 95/05 and 92 °C for PBMPsu 90/10, respectively), and held for another 2 min to yield suitably sized spherulites. Then, a scan to room temperature at a cooling rate of 1, 2.5 or 5 °C/min was conducted for subsequent analysis. The final pictures of these specimens were taken using digital camera. In the isothermal experiments, the premolten specimen was cooled rapidly to the specific crystallization temperature (T_c), which ranged from 97 °C to 75 °C. The sizes of the spherulites during crystallization were recorded versus time, and the growth rates of the spherulites were calculated from the slopes of the plots of radius versus time.

Measuring DSC

A TA instrument DSC 2910 with a refrigerating system was used to investigate the nonisothermal crystallization of these polyesters from the melt state under a dynamic

atmosphere of nitrogen at 50 ml/min. Approximately 10 mg of fresh sample was used in each case. The samples started from 30 °C up to 190 °C at a heating rate of 10 °C/min and held for 5 min to eliminate thermal history. Then the samples were cooled down to 10 °C at a rate of 1, 2.5, 5, 10 or 20 °C/min, respectively. The exothermic crystallization curves were recorded as a function of temperature or time, and the nonisothermal crystallization kinetics was analyzed by different models [34–41].

Results and discussion

Determination of growth rates by the non-isothermal method

In general, the growth rate (G) of spherulites is determined by measuring the spherulitic radii (r) from PLM micrographs that are taken at time (t) intervals before spherulitic impingement during the isothermal crystallization experiments. Although this method is easy and accurate, it is time consuming. The nonisothermal method for estimating the G values of polymers is an alternative means of solving this problem. Combining self-nucleation and nonisothermal temperature programs [42–45] widens the range of temperatures (T) over which the growth rate can be measured.

When the melt of the specimen is solidified at a constant cooling rate (dT/dt , ϕ), the G values can be estimated from the following equation:

$$G = \frac{dr}{dt} = \frac{dr}{dT} \frac{dT}{dt} = \frac{dr}{dT} \phi \quad (1)$$

Different cooling rates were used to determine the growth rates of PBSu and its copolymers. Slower cooling rate allows G to be measured over a narrow range near higher T_c . In the contrast, faster cooling rate can be applied to a wider T_c range. Figure 2 displays the crystal growth rates of PBMPsu 90/10 obtained by nonisothermal crystallization at cooling rates at 1, 2.5 or 5 °C/min. These three continuous curves are in good agreement. Properly fitting these three curves from different cooling rates gives a curve for the growth rate vs. temperature, which is shown as a short dash line in Fig. 3. The other two curves for PBSu and PBMPsu 95/05 are also plotted in Fig. 3 for comparison. The growth rates of spherulite for PBMPsu 90/10 increase from 0.02 $\mu\text{m/s}$ at 92 °C to a value of 0.3 $\mu\text{m/s}$ at 74 °C. The growth rate of spherulite for PBMPsu 90/10 is the lowest and that for PBSu is the highest. It reveals that the growth rate decreases gradually with the amount of minor MS units incorporated into PBSu. Symbol points in Fig. 3 were obtained under the isothermal crystallization experiments at various T_c values. It can be found that the growth rates of spherulite measured using isothermal method are very close to those results obtained using nonisothermal method. The maximum growth rate of these polyesters can not be observed because the crystallization rate of them is too fast to be measured. The growth rate of PBMPsu 90/10 spherulites is about one ninth of that of PBSu at 82 °C; that of PBMPsu 95/05 is about one third

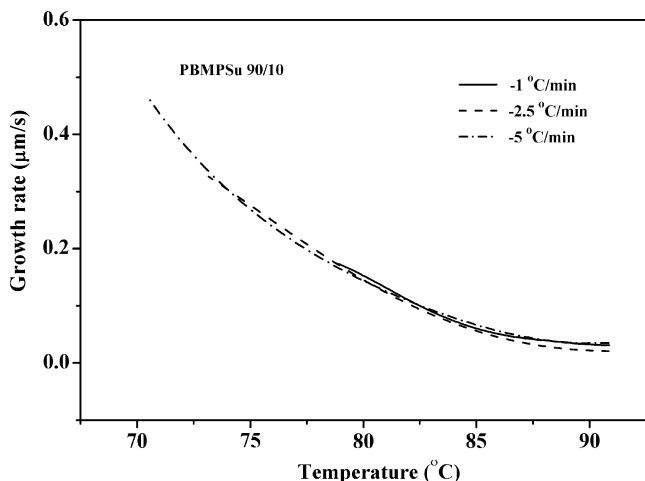


Fig. 2 Spherulitic growth rates of PBMPsu 90/10 during cooling at various rates

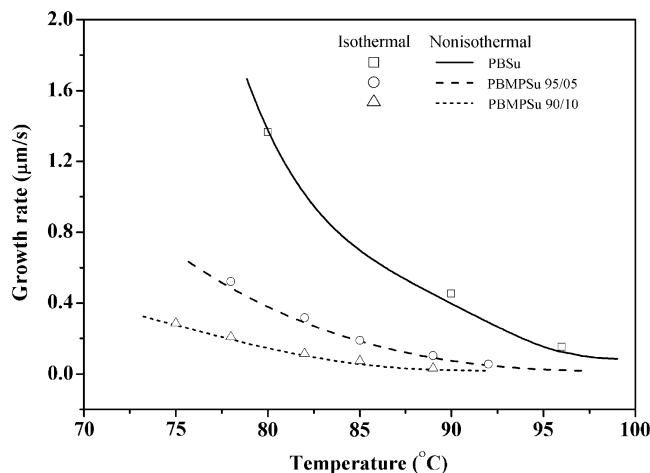


Fig. 3 Spherulitic growth rates for three kinds of polyesters by using nonisothermal method and under isothermal conditions

of PBSu. These results reveal that an efficient and reliable non-isothermal method can be adopted to obtain the isothermal growth rate of spherulites.

Kinetic analysis of growth rates of spherulites

Based on the secondary nucleation theory of LH [32], the growth rates of spherulites can be expressed as

$$G = G_0 \exp\left[\frac{-U^*}{R(T_c - T_\infty)}\right] \exp\left[\frac{-K_g}{T_c(\Delta T)f}\right] \quad (2)$$

where G_0 denotes a preexponential factor, R represents the gas constant; U^* is the activation energy of reptational diffusion; K_g denotes the nucleation parameter, T_∞ is a hypothetical temperature below which motion ceases; $\Delta T = (T_m^o - T_c)$ indicates the degree of undercooling, T_m^o is the equilibrium melting temperature, and f is a correction term of the order of unity, and is usually given by $f = 2T_c/(T_m^o + T_c)$. The continuous growth rate data in Fig. 3 was analyzed using Eq. 2. The regime transition analyses of the LH model were performed by both empirical ($U^*=1,500$ cal/mol, $T_\infty=T_g-30$) and Williams-Landel-Ferry (WLF) ($U^*=4,200$ cal/mol, $T_\infty=T_g-51.6$) values, respectively, as shown in Table 1. Figure 4 presents a typical regime analysis using the following values; $U^*=35,000$ cal/mol and $T_\infty=T_g-30$ K with T_g at 234.8 K. $T_m^o=391.5$ K [Supporting Information Fig. S1] was used. The two optimally fit lines of $\log G + U^*/[2.303R(T_c - T_\infty)]$ as a function of $1/(T_c\Delta T f)$ yield the values of K_g (slope $\times 2.303$) and $\log G_0$ (intercept) in each regime for PBMPsu 90/10. A break in the curve occurs at $T_c=77.9$ °C and the ratio of the two slopes is 2.0, as shown in the 17th row of Table 1. Columns 4–9 in Table 1 present the calculated values of K_g , the correlation coefficient (r^2) and

Table 1 Values of K_g , correlation coefficient and transition temperature determined from secondary nucleation theory using the continuous growth rates of nonisothermal method

Sample	T_∞ (K)	U^* (cal/mol)	$K_g(\text{III}) \times 10^{-5}$ (K ²)	$r^2(\text{III})$	$K_g(\text{II}) \times 10^{-5}$ (K ²)	$r^2(\text{II})$	$K_g(\text{III})/K_g(\text{II})$	$T_{\text{II} \rightarrow \text{III}}$ (°C)
PBSu	T_g -30	1,000	1.31	0.9982	0.68	0.9755	1.94	96.2
	T_g -30	1,500	1.37	0.9985	0.72	0.9782	1.91	96.2
	T_g -30	6,500	1.97	0.9998	1.17	0.9909	1.68	96.0
	T_g -51.6	2,000	1.38	0.9985	0.72	0.9786	1.90	96.2
	T_g -51.6	3,000	1.47	0.9989	0.79	0.9819	1.85	96.2
	T_g -51.6	4,200	1.58	0.9992	0.88	0.9849	1.79	96.1
PBMPsu 95/5	T_g -30	1,500	1.21	0.9992	0.94	0.9985	1.23	84.0
	T_g -30	6,500	2.13	0.9974	1.35	0.9970	1.53	83.7
	T_g -30	17,000	4.06	0.9958	2.20	0.9953	1.84	83.6
	T_g -30	34,000	7.18	0.9949	3.59	0.9940	2.00	83.5
	T_g -51.6	4,200	1.53	0.9986	1.08	0.9980	1.41	83.8
	T_g -51.6	17,000	3.31	0.9964	1.89	0.9959	1.75	83.6
	T_g -51.6	37,000	6.22	0.9959	3.11	0.9950	2.00	83.5
	PBMPsu 90/10	T_g -30	1,500	1.32	0.9984	0.93	0.9987	1.42
T_g -30		6,500	2.37	0.9981	1.47	0.9970	1.62	77.2
T_g -30		17,000	4.57	0.9979	2.59	0.9952	1.77	77.7
T_g -30		35,000	8.54	0.9983	4.28	0.9923	2.00	77.9
T_g -51.6		4,200	1.67	0.9983	1.12	0.9981	1.50	77.2
T_g -51.6		17,000	3.69	0.9980	2.16	0.9958	1.71	77.7
T_g -51.6		37,000	6.85	0.9979	3.79	0.9945	1.81	77.8

regime II→III transition temperature ($T_{\text{II} \rightarrow \text{III}}$) as for various T_∞ and U^* values (see columns 2 and 3). It is obvious that the regime transition temperature $T_{\text{II} \rightarrow \text{III}}$ is almost independent of the values of U^* for each sample. The results show that $T_{\text{II} \rightarrow \text{III}}$ is 96.2, 83.5, and 77.9 °C for PBSu, PBMPsu 95/05, and PBMPsu 90/10, respectively. The $T_{\text{II} \rightarrow \text{III}}$ for PBSu crystallization is very close to the value 96 °C in the literature [9, 23].

Morphology of spherulites

Figure 5 shows micrographs of PBSu, PBMPsu 95/05, and PBMPsu 90/10 that had been crystallized from the melt at cooling rates of 1 and 5 °C/min. The spherulite size increased as the cooling rate declined because the nucleation rate decreased, reducing the nucleation density. These spherulites displayed Maltese cross. Bands were observed at regular intervals in the radial direction in the extinction patterns of the PBSu spherulites and those copolyesters spherulites. The textures of the ringed band spherulites become more obvious as the cooling rate or the amount of MS units increases. The spacing between the ringed bands decreased as the cooling rate increased, while those near the center of the spherulites increased because of the slower growth rate at a higher temperature. It is well known that ringed bands are often found in many semicrystalline polymers and are produced by the periodic twisting of radiating lamellar crystals about their axes of fastest growth [46]. The spherulites of PBSu homopolymers are larger than those of these copolyesters, as revealed by the textures of Fig. 5. It indicated that incorporating minor MS units into PBSu substantially inhibits the crystallization behavior of PBSu, leading to a clear secondary crystallization phenomenon.

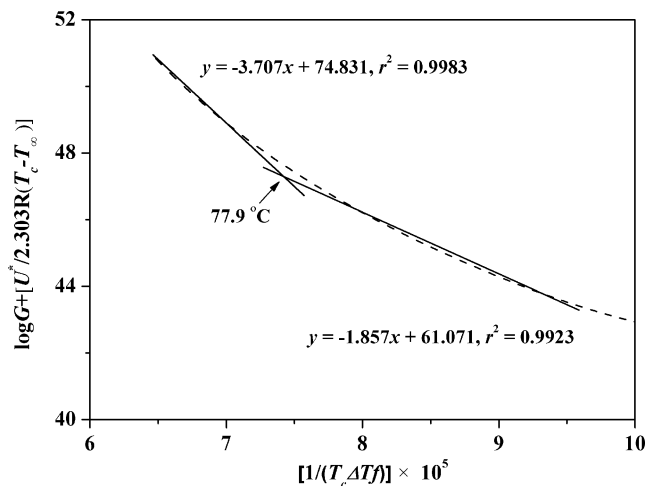
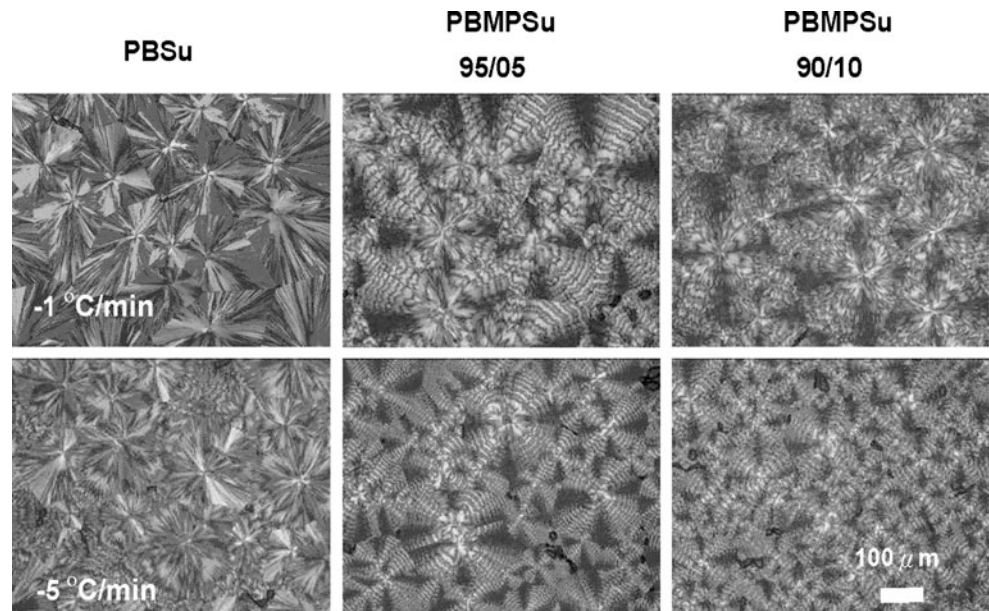


Fig. 4 Kinetic analysis of the continuous growth rate data of PBMPsu 90/10. In this case, $U^*=35,000$ cal/mol, and $T_\infty=T_g-30$ K

Fig. 5 Representative PLM micrographs of PBSu, PBMPsu 95/05 and PBMPsu 90/10 non-isothermal crystallized at the cooling rate of 1 °C/min (upper) and 5 °C/min (lower). The scale bar at the lower right is the same for all photos



Nonisothermal crystallization

Figure 6 presents the nonisothermal melt-exothermic curves of PBMPsu90/10 recorded at five different cooling rates from 1 to 20 °C/min. It is apparent that these exothermic curves become broader and shift to the lower temperature region as the cooling rate increases. The times and temperatures of the starting, peak and ending of these nonisothermal exothermic curves were recorded. Table 2 lists the basic parameters of these polyesters, such as the peak temperature (T_p) and the enthalpy of nonisothermal crystallization (ΔH_c). The values of T_p or ΔH_c decreased as the cooling rate increased in each case and they followed the order of PBSu > PBMPsu 95/05 > PBMPsu 90/10 at a given cooling rate. Figure 7 displays a time-temperature-

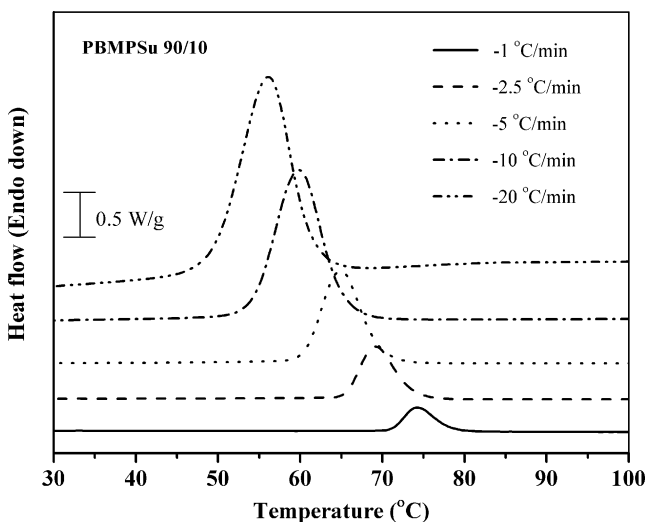


Fig. 6 DSC traces of PBMPsu 90/10 at various cooling rates

transformation (TTT) diagram superposed on the continuous-cooling-transformation (CCT) curves for PBMPsu 90/10 samples following the consolidation at 190 °C for 5 min. The CCT curves plot the value of temperature versus crystallization time (in unit min) at the five cooling rates. The TTT diagram is established by fitting the connecting points of the starting, peak and ending times for the nonisothermal crystallization processes. Based on the kinetic analysis of the growth rates of PBMPsu 90/10 spherulites in the previous section, it shows that $T_{II \rightarrow III}$ is 77.9 °C (a horizontal dash line), which exceeded the starting temperatures of nonisothermal crystallization, except $T_{II \rightarrow III}$ was only a few degrees below the starting temperatures at the cooling rates of 1 and 2.5 °C/min, as shown in Fig. 7. It indicates that most of the nonisothermal crystallization of PBMPsu 90/10 in this study occurred in regime III. PBSu and PBMPsu 95/05 had all of the nonisothermal crystallization occurred in regime III. In regime III, the crystallization rate is relatively high, and the polymer chains do not undergo repeated adjacent reentry into the lamellae [47]. The secondary crystallization may be more likely to occur in regime III than in regime II.

From the DSC thermograms in Fig. 6, the relative degree of crystallinity, X_T , at various cooling rates can be expressed as a function of temperature (T) based on the following equation:

$$X_T = \int_{T_0}^T \frac{dH}{dT} dT / \int_{T_0}^{T_\infty} \frac{dH}{dT} dT \quad (3)$$

where dH denotes the enthalpy of crystallization released during an infinitesimal temperature interval dT , T_0 and T_∞ are the starting and ending temperatures of nonisothermal

Table 2 Kinetics parameters of nonisothermal crystallization based on the modified Avrami equation

Sample	ϕ (°C/min)	n	K_c (min ⁻ⁿ)	$t_{1/2}$ (min)	Peak temp. (°C)	ΔH_c (J/g)	X_c^a (%)
PBSu	-1	3.9	2.92×10^{-4}	7.6	89.4	75.2	35.8
	-2.5	4.1	1.16×10^{-1}	3.4	85.1	73.5	35.0
	-5	4.4	5.92×10^{-1}	1.8	81.7	70.5	33.6
	-10	3.9	9.10×10^{-1}	1.0	77.5	69.3	33.0
	-20	3.7	1.11	0.5	72.1	66.3	31.6
PBMPsu 95/05	-1	4.0	2.44×10^{-4}	7.8	76.8	65.6	31.3
	-2.5	4.4	9.73×10^{-2}	3.7	72.3	64.4	30.6
	-5	4.0	5.79×10^{-1}	1.9	68.0	63.2	30.1
	-10	4.8	8.51×10^{-1}	1.2	63.8	62.8	29.9
	-20	3.4	1.09	0.5	59.6	61.9	29.5
PBMPsu 90/10	-1	4.0	1.09×10^{-4}	8.7	74.3	61.5	29.3
	-2.5	4.2	9.45×10^{-2}	3.8	69.2	61.2	29.1
	-5	4.2	5.09×10^{-1}	2.0	64.9	60.7	28.9
	-10	4.4	8.38×10^{-1}	1.3	59.9	60.3	28.7
	-20	3.4	1.07	0.6	56.1	58.6	27.9

^a Enthalpy of fusion of PBSu is 210 J/g [14]

crystallization. The temperature abscissa can be transformed into a time scale, as shown in Fig. 8, based on the equation of $t=(T_0-T)/\phi$, where T is the temperature at crystallization time t , and ϕ is the cooling rate. X_T is replaced by X_t after the transformation of abscissa from T to t . The half-time of crystallization ($t_{1/2}$ —defined as the time required from the starting of crystallization to the time at which X_t is 50%) was evaluated. Figure 8 and $t_{1/2}$ values in Table 2 indicate that increasing the cooling rate reduces the crystallization time. Column 7 in Table 2 shows the enthalpy of nonisothermal crystallization (ΔH_c), which average value declines from 71.0 ± 3.5 J/g for PBSu, through 63.6 ± 1.4 J/g for PBMPsu 95/05, to 60.5 ± 1.1 J/g

for PBMPsu 90/10. The degree of crystallinity was calculated by dividing ΔH_c by 210 J/g [14], and is listed in the last column in Table 2. Incorporating minor 6.5 or 10.8 mol% MS units into PBSu markedly inhibits the crystallization behavior of PBSu, therefore, the secondary crystallization behavior in the copolymers cannot be ignored.

Avrami model

The most common model to describe the overall isothermal crystallization kinetics is the Avrami equation [34, 35]. It assumes that the development of the relative

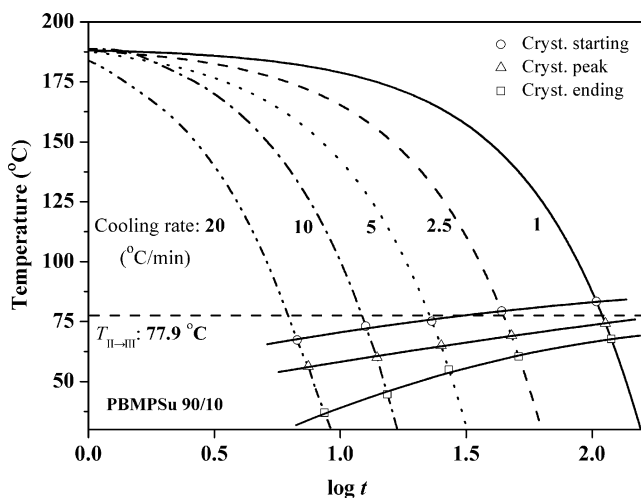


Fig. 7 A time-temperature-transformation (TTT) diagram superposed on the continuous-cooling-transformation (CCT) curves for PBMPsu 90/10. T_{II-III} is regime II→III transition temperature

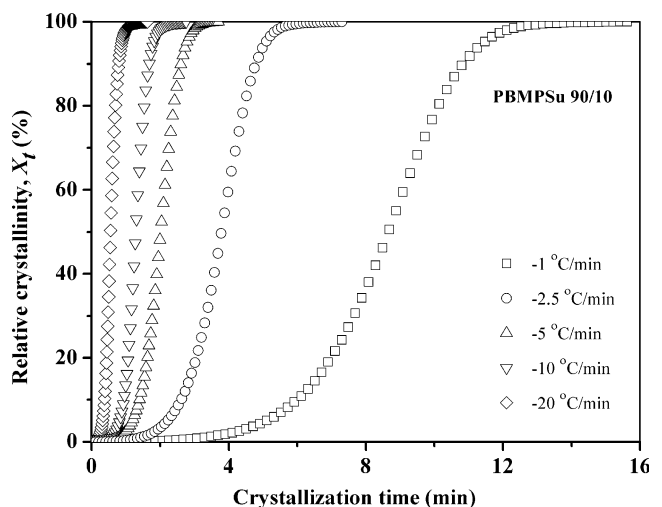


Fig. 8 Relative crystallinity as a function of time for PBMPsu 90/10 at various cooling rates

degree of crystallinity, X_t , is related to the crystallization time t as,

$$1 - X_t = \exp(-Kt^n) \quad (4)$$

Taking the double-logarithms form as follows:

$$\log[-\ln(1 - X_t)] = \log K + n \log t \quad (5)$$

where K and n are the crystallization rate constant and Avrami exponent, respectively. Avrami equation has been modified by Jeziorny. He proposed a method to determine the parameters characterizing the kinetics of nonisothermal crystallization [36]. Assuming constant cooling rate (ϕ), the final form is given as:

$$\log K_c = \log K / \phi \quad (6)$$

Given Eq. 5, Fig. 9 shows the plots of Avrami model with time in unit min. In the fitting, the relative crystallinity data between 0.5% and 99.5% were used. The slope and the intercept yield the values of the Avrami exponent n and the rate parameter K (K_c from Eq. 6), which are given in Table 2. The n values were found to be in the range of 3.7~4.4, 3.4~4.8 and 3.4~4.4 for PBSu, PBMPsu 95/05, and PBMPsu 90/10, respectively, suggesting that the crystallization proceeds by three-dimension spherical growth. The values of K_c increased as the cooling rate increased. However, in nonisothermal crystallization, K_c and n do not have the same physical significance as in the isothermal process because the temperature decreases continuously in a nonisothermal process. This change in temperature affects the rate of both nuclei formation and spherulite growth. Based on the values of K_c and $t_{1/2}$, as

shown in Table 2, the crystallization rate followed the order: PBSu > PBMPsu 95/05 > PBMPsu 90/10. In this study, the possible effect of molecular weight on the growth rate and the overall crystallization rate of these polyesters are not discussed because the intrinsic viscosity, \bar{M}_n and molecular weight distribution of these polyesters were close to each other [31].

Ozawa model

When the time variable in the Avrami equation was replaced by a cooling rate (by replacing t with T/ϕ), Ozawa [37] model can be expressed as follows:

$$1 - X_t = \exp[-K(T)/\phi^m] \quad (7)$$

Taking the double logarithm of Eq. 7 and rearranging yields the following form

$$\log[-\ln(1 - X_t)] = \log K(T) - m \log \phi \quad (8)$$

where $K(T)$ is a function of the cooling rate, and m is an Ozawa exponent. A plot of $\log[-\ln(1 - X_t)]$ versus $\log \phi$ at a given temperature should be a straight line if the Ozawa equation captures the nonisothermal crystallization process very well. $K(T)$ and m are obtained from the intercept and the slope, respectively. According to the Ozawa model, the analyses of the data within the temperatures ranging from 63 to 73 °C are shown in Fig. 10 for PBMPsu 90/10. The plots of $\log[-\ln(1 - X_t)]$ against $\log \phi$ are not straight lines. Evidently, the Ozawa analysis does not accurately describe the nonisothermal crystallization kinetics of this copolyester because part of the crystallization is secondary crystallization, as discussed in the previous sections. Similar results

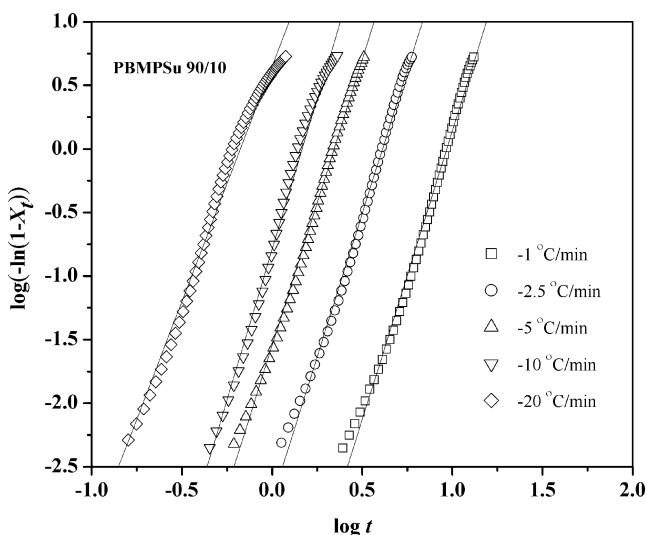


Fig. 9 Avrami plots for nonisothermal crystallization of PBMPsu 90/10

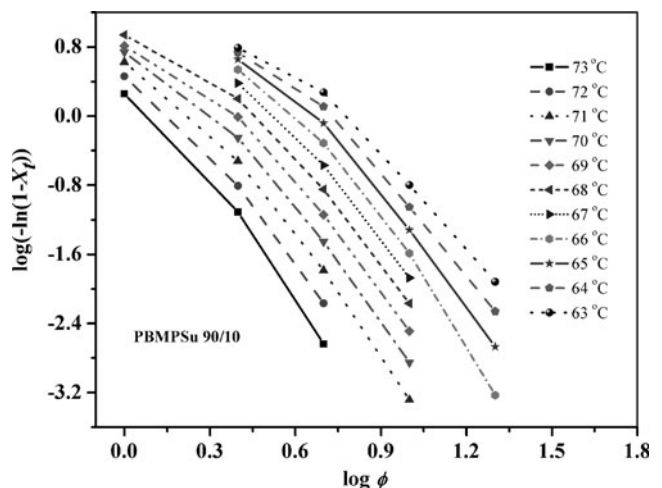


Fig. 10 Ozawa plots for nonisothermal crystallization of PBMPsu 90/10

are obtained for PBSu and PBMPsu 95/05, and are consistent with the result for PBSu in the literature [48].

Mo model

Mo and coworkers [38] proposed a different approach for the nonisothermal crystallization by combining the Avrami equation with the Ozawa equation as below:

$$\log K + n \log t = \log K(T) - m \log \phi \tag{9}$$

or equivalently

$$\log \phi = \log F(T) - a \log t \tag{10}$$

where the parameter $F(T) = [K(T)/K]^{1/m}$, a is the ratio of the Avrami exponent n to the Ozawa exponent m , i.e., $a = n / m$. According to the Mo method, at a given degree of crystallinity, the plot of $\log \phi$ versus $\log t$ should yield a straight line, as presented in Fig. 11 for PBMPsu 90/10. It is clear that Mo model describes the nonisothermal crystallization of PBMPsu 90/10 well with the correlation coefficient values larger than 0.995. The kinetic parameter $F(T)$ and a value can be determined from the intercept and the slope, respectively. Table 3 lists the values of $F(T)$ and a for PBSu, PBMPsu 95/05 and PBMPsu 90/10, respectively. The value of $F(T)$ increases with increasing the degree of crystallinity, which indicated that at unit crystallization time, a higher cooling rate is required to reach a higher X_t . To have the same X_t , the required cooling rate followed the order: PBMPsu 90/10 > PBMPsu 95/05 > PBSu. This result reveals that the crystallization rate followed the order: PBSu > PBMPsu 95/05 > PBMPsu 90/10, again. The value of a exceeds 1, indicating that n is always larger than

m , and suggesting that markedly secondary crystallization growth accompanies primary crystallization during the nonisothermal crystallization.

Effective activation energy

Kissinger’s method [49] has been adopted frequently for evaluating the effective activation energy during non-isothermal crystallization. This method has been formulated for heating experiments, but it has been demonstrated by Vyazovkin et al. that dropping the negative sign for the rate parameter (i.e., cooling rate) is a mathematically invalid procedure [40, 41]. The differential isoconversional method of Friedman [39] is as follows:

$$\ln(dX_t/dt) = A - \Delta E_{X_t}/RT_{X_t} \tag{11}$$

where dX_t/dt represents the instantaneous crystallization rate as a function of time for a given value of X_t , A is a preexponential constant, and ΔE_{X_t} denotes the effective energy barrier in the process for a given X_t . Plotting $\ln(dX_t/dt)$ versus $1/T_{X_t}$ at a given degree of relative crystallinity (X_t) yields a straight line with a slope of $-\Delta E_{X_t}/R$. Figure 12 plots the dependence of the effective activation energy on the relative degree of crystallinity. ΔE_{X_t} was found to increase with the relative crystallinity in these three polyesters, suggesting that as the crystallization proceeded polymer became more difficult to be crystallized. The values of ΔE_{X_t} for PBSu, PBMPsu 95/05 and PBMPsu 90/10 were -180.3 , -161.9 and -149.3 kJ/mol, respectively, at a given value of $X_t=10\%$. At all X_t values, ΔE_{X_t} followed the order: PBSu < PBMPsu 95/5 < PBMPsu 90/10.

The effective activation energy can be determined by the advanced integral isoconversional method of Vyazovkin

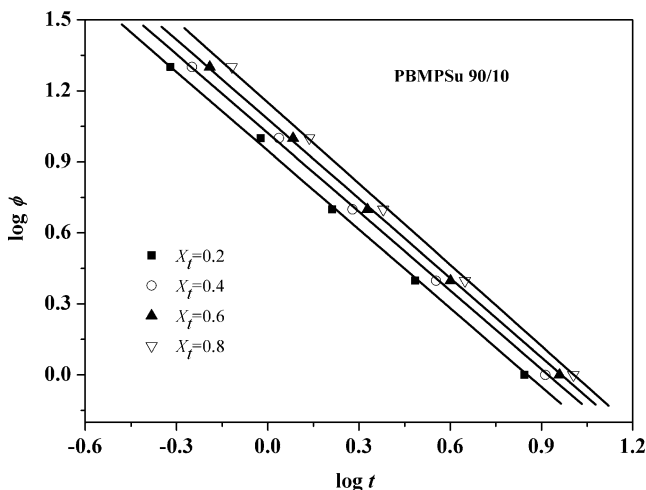


Fig. 11 Log ϕ versus $\log t$ at different relative degrees of crystallinity for PBMPsu 90/10

Table 3 Values of $F(T)$ and a versus relative degree of crystallinity based on Mo’s treatment

Sample	X_t (%)	$F(T)$	a (=n/m)	r^2
PBSu	20	7.85	1.14	1.000
	40	9.36	1.13	1.000
	60	10.86	1.15	1.000
	80	13.07	1.17	1.000
PBMPsu 95/05	20	7.90	1.10	0.991
	40	9.39	1.10	0.993
	60	10.88	1.12	0.994
	80	13.11	1.15	0.996
PBMPsu 90/10	20	8.86	1.11	0.995
	40	10.51	1.11	0.996
	60	12.03	1.12	0.997
	80	14.16	1.14	0.998

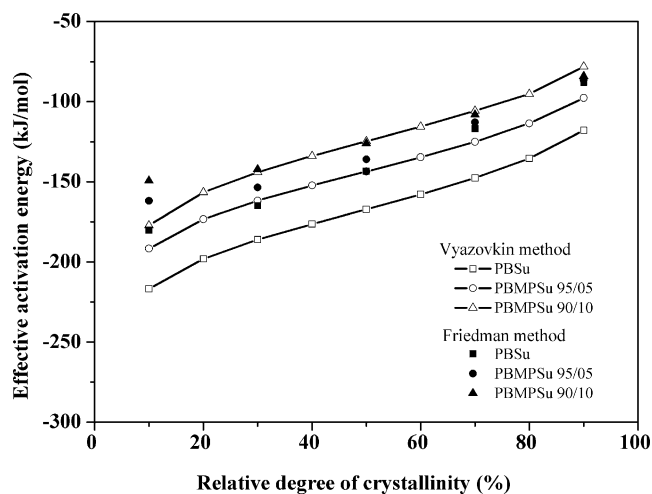


Fig. 12 Dependence of the effective activation energy on the relative degree of crystallinity from Vyazovkin's and Fridman's methods

[40, 41]. According to Vyazovkin's method, the temperature dependence of the effective activation energy (ΔE_T) of the growth rate (G) is calculated as follows:

$$\Delta E_T = -R \frac{d(\ln G)}{d(1/T)} = U^* \frac{T^2}{(T - T_\infty)^2} + K_g R \times \frac{(T_m^0)^2 - T^2 - T_m^0 T}{(T_m^0 - T)^2 T} \quad (12)$$

Activation energy (ΔE_T) can be obtained using the values of $G \approx 1/t_{1/2}$ from nonisothermal crystallization experiment [50]. There is a temperature corresponding to $t_{1/2}$ from the DSC experiment for each cooling rate (see Table 2). According to Eq. 2, the value of K_g for Vyazovkin equation can be obtained by five data points which were analyzed using the following values: $U^* = 6,500$ cal/mol and $T_\infty = T_g - 30$ K for PBSu, PBMPsu 95/05 and PBMPsu 90/10, respectively. The values of ΔE_T can be then calculated from Eq. 12 using these values of K_g and U^* . Figure 12 plots the conversion dependence of the effective activation energy (ΔE_T) from the Fridman and Vyazovkin methods for comparison. Figure 13 presents the temperature dependence of these ΔE_T values from both methods. The values of ΔE_T for PBMPsu 90/10 using Fridman method are very close to those values using Vyazovkin method. The values of ΔE_T for PBSu were always smaller than those for the other two at the same conversion and followed the order: PBSu < PBMPsu 95/5 < PBMPsu 90/10. This result is in consistent with the analyses of Friedman model and the measured growth rates of these polyesters, as described above. It reveals that incorporating minor MS units into PBSu will result in a lower crystallinity and increase its biodegradability.

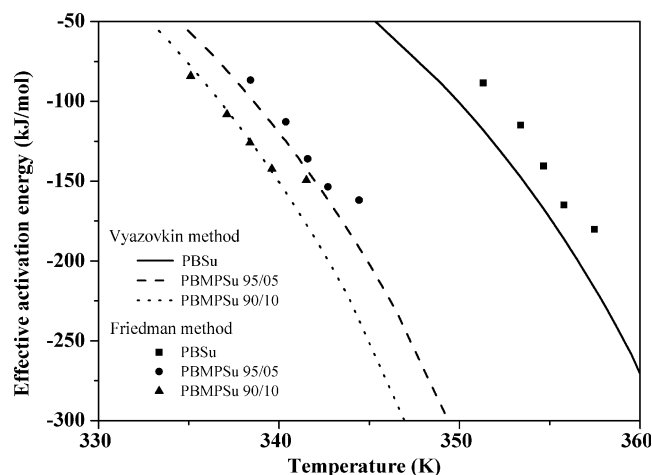


Fig. 13 Dependence of the effective activation energy on the temperature from Vyazovkin's and Fridman's methods

Conclusions

PBSu and two PBMPsu copolymers with high molecular weights were studied. The compositions of the PBMPsu 95/05 and PBMPsu 90/10 were characterized as having 6.5 and 10.8 mol% MS units, respectively. The isothermal growth rates of spherulites were determined using the nonisothermal method at cooling rates of 1, 2.5 and 5 °C/min, respectively. This method is efficient and reliable comparing with the isothermal method because the values of growth rates from the nonisothermal method fit very well with the values from the isothermal experiments. The growth rate of spherulites for PBMPsu 90/10 copolyester was about one ninth of that for PBSu, and that for PBMPsu 95/05 was about one third of that for PBSu at 82 °C. This result reveals that incorporating minor amount of MS units into the backbone of PBSu homopolymer substantially decreased the crystallization rate of the resulting copolymer. Based on the Hoffman–Lauritzen theory, the regime II→III transition temperatures of PBSu, PBMPsu 95/05 and PBMPsu 90/10 occurred at about 96.2, 83.5 and 77.9 °C, respectively.

Nonisothermal crystallization kinetics of neat PBSu and PBMPsu copolymers were investigated by DSC. The values of crystallization rates were found to be of the following order at a given cooling rate: PBSu > PBMPsu 95/05 > PBMPsu 90/10. The results indicated that the crystallization of PBSu copolyesters with minor amount MS units were retarded comparing with that of neat PBSu. The modified Avrami and Mo models were found to provide a good fit to the experimental data in this study. The results of kinetic analysis of these polyesters from the rate parameter K_c (from the modified Avrami model), the kinetic parameter $F(T)$ (from the Mo model), and the crystallization activation energies (from the Friedman and

Vyazovkin models) give the same demonstration that neat PBSu was more crystallizable than its copolymers. The results of both PLM and DSC experiments reveal that the crystallization rate and the degree of crystallinity of PBMPsu decrease as the mole% of MS unit increases.

Acknowledgements The authors thank the National Science Council of the Republic of China, Taiwan, for financially supporting this research under Contract No. NSC 98-2221-E-110-007.

References

1. Mochizuki M, Hirami M (1997) *Polym Adv Technol* 8:203–209
2. Ishioka R, Kitakuni E, Ichikawa Y (2002) *Biopolymers*, vol 4. Wiley-VCH, pp 275–297
3. Kumagai Y, Kanesawa Y, Doi Y (1992) *Macromol Chem Phys* 193:53–57
4. Chatani Y, Hasegawa R, Tadokoro H (1971) *Polym Prepr Jpn* 20:420
5. Ichikawa Y, Suzuki J, Washiyama J, Moteki Y, Noguchi K, Okuyama K (1995) *Polymer J* 27:1230–1238
6. Ihn KJ, Yoo ES, Im SS (1995) *Macromolecules* 28:2460–2464
7. Miyata T, Masuko T (1998) *Polymer* 39:1399–1401
8. Yoo ES, Im SS (1999) *J Polym Sci Part B: Polym Phys* 37:1357–1366
9. Gan ZH, Abe H, Kurokawa H, Doi Y (2001) *Biomacromolecules* 2:605–613
10. Cao A, Okamura T, Nakayama K (2002) *Polym Degrad Stab* 78:107–117
11. Yasuniwa M, Satou T (2002) *J Polym Sci Part B: Polym Phys* 40:2411–2420
12. Qiu ZB, Komura M, Ikehara T, Nishi T (2003) *Polymer* 44:7781–7785
13. Yasuniwa M, Tsubakihara S, Satou T, Iura K (2005) *J Polym Sci Part B: Polym Phys* 43:2039–2047
14. Papageorgiou GZ, Bikiaris DN (2005) *Polymer* 46:12081–12092
15. Wang XH, Zhou JJ, Li L (2007) *Eur Polym J* 43:3163–3170
16. Zhu CY, Zhang ZG, Liu QP, Wang ZP, Jin J (2003) *J Appl Polym Sci* 90:982–990
17. Tserki V, Matzinos P, Pavlidou E, Vachliotis D, Panayiotou C (2006) *Polym Degrad Stab* 91:367–376
18. Ranucci E, Liu Y, Lindblad MS, Albertsson AC (2000) *Macromol Rapid Commun* 21:680–684
19. Liu Y, Ranucci E, Lindblad MS, Albertsson AC (2001) *J Polym Sci Part A: Polym Chem* 39:2508–2519
20. Chrissafis K, Paraskevopoulos KM, Bikiaris DN (2006) *Polym Degrad Stab* 91:60–68
21. Xu YX, Xu J, Guo BH, Xie XM (2007) *J Polym Sci Part B: Polym Phys* 45:420–428
22. Xu YX, Wu J, Liu DH, Guo BH, Xie XM (2008) *J Appl Polym Sci* 109:1881–1889
23. Papageorgiou GZ, Bikiaris DN (2007) *Biomacromolecules* 8:2437–2449
24. Chen CH, Peng JS, Chen M, Lu HY, Tsai CJ, Yang CS (2010) *Colloid Polym Sci* 288:731–738
25. Lu SF, Chen M, Shih YC, Chen CH (2010) *J Polym Sci Part B: Polym Phys* 48:1299–1308
26. Sullivan CJ, Dehm DC, Reich EE, Dillon ME (1990) *J Coat Technol* 62:37–45
27. Bello P, Bello A, Riande E (1999) *Macromolecules* 32:8197–8203
28. Nalampang K, Johnson AF (2003) *Polymer* 44:6103–6109
29. Suh J, Spruiell JE, Schwartz SA (2003) *J Appl Polym Sci* 88:2598–2606
30. Lewis CL, Spruiell JE (2006) *J Appl Polym Sci* 100:2592–2603
31. Chen CH, Yang CS, Chen M, Shih YC, Hsu HS, Lu SF (2010) *eXPRESS Polym Lett*. doi:10.3144/expresspolymlett.2011.29
32. Hoffman JD, Davis GT, Lauritzen JI Jr (1976) *Treatise on solid state chemistry*, Vol 3, Chapter 7. Plenum, New York
33. Chen M, Chung CT (1998) *Polym Compos* 19:689–697
34. Avrami M (1940) *J Chem Phys* 8:212–224
35. Avrami M (1941) *J Chem Phys* 9:177–184
36. Jeziorny A (1978) *Polymer* 19:1142–1144
37. Ozawa T (1971) *Polymer* 12:150–158
38. Liu TX, Mo ZS, Wang SG, Zhang HF (1997) *Polym Eng Sci* 37:568–575
39. Friedman HL (1964) *J Polym Sci Part C* 6:183–195
40. Vyazovkin S (2001) *J Comput Chem* 22:178–183
41. Vyazovkin S, Sbirrazzuoli N (2004) *Macromol Rapid Commun* 25:733–738
42. Chung CT, Chen M (1992) *Polym Prepr* 33:420–421
43. Chen M, Chung CT (1998) *J Polym Sci Part B: Polym Phys* 36:2393–2399
44. Di Lorenzo ML, Cimmino S, Silvestre C (2000) *Macromolecules* 33:3828–3832
45. Tsai CJ, Chen M, Lu HY, Chang WC, Chen CH (2010) *J Polym Sci Part B: Polym Phys* 48:932–939
46. Keller A (1955) *J Polym Sci* 17:351–364
47. Sperling LH (2006) *Introduction to physical polymer science*, 4th ed, chapter 6. Wiley-Interscience, New York
48. Qiu ZB, Fujinami S, Komura M, Nakajima K, Ikehara T, Nishi T (2004) *Polym J* 36:642–646
49. Kissinger HE (1957) *Anal Chem* 29:1702–1706
50. Papageorgiou GZ, Achilias DS, Bikiaris DN (2007) *Macromol Chem Phys* 208:1250–1264